Local Model Network based Dynamic Battery Cell Model Identification

CHRISTOPH HAMETNER, JOHANNES UNGER AND STEFAN JAKUBEK
Christian Doppler Laboratory for Model Based Calibration Methodologies
Vienna University of Technology
Wiedner Hauptstrasse 8-10, 1040 Vienna
AUSTRIA
christoph.hametner@tuwien.ac.at, johannes.unger@tuwien.ac.at, stefan.jakubek@tuwien.ac.at

Abstract: In this paper the local model network (LMN) based dynamic battery cell model identification is presented. Such a model describes the nonlinear dynamic behaviour of the cell terminal voltage in dependance of the charge/discharge current and can be used for the state of charge (SoC) estimation in hybrid electrical vehicles. For that purpose, the model must be accurate at high C-rates in combination with a highly dynamic excitation. The LMN construction, related SoC observer structures and the appropriate experiment design are discussed in the present paper. The proposed concepts and the performance of the LMN is validated by means of real measurement data from a Lithium Ion power cell.

Key–Words: Nonlinear system identification, local model network, battery cell modelling, state of charge estimation

1 Introduction

The *traction battery* in a hybrid electric vehicle (HEV) is a complex system consisting of many single cells and an especially designed electrical/electronical circuit. Part of that circuit - and by far the most critical due to its complicated calibration - is the *battery management system (BMS)*. This supervising control unit processes the actual status of the cells of the traction battery and shares the computed data set with the rest of the vehicle's controllers (in particular with the *hybrid control unit, HCU*). It determines the major operational tasks of the traction battery as are available power and energy, high reliability (long cycle and long calendar life), and battery safety under any circumstances (i. e. use and abuse cases). Achieving these goals is widely connected to the quality of the battery management system and its interaction with the other vehicle control units, [17, 6].

The correct determination of the *state-of charge (SoC)* and also the related state of power are addressed as the most important calibration tasks of the BMS. An integral part of the BMS is a mathematical cell model which allows to predict the nonlinear system dynamics of the traction battery under the specific loads and environmental conditions, since it is not possible to measure the state of charge directly.

In this paper the nonlinear system identification of a Lithium Ion cell for the purpose of SoC estimation is presented. In the following, the requirements for the cell model for the application in HEV development are formulated (c. f. [21]):

- based only on readily available signals only (cell terminal voltage, cell current, cell external temperature),
- valid up to very high C-rates ($\pm 20C$),
- highly accurate even under strong dynamic excitation,
- includes special effects such as hysteresis and relaxation,
- suitable for real-time applications.

Typical modelling approaches in the field of battery cell modelling are:

- *Electro-chemical modelling:* These models are based on a detailed electro-chemical description of the cell, see e. g. [2, 16, 7]. The major disadvantages of this approach are that the time efficient parametrisation as well as the real-time application is very complex or even not possible.
- *Equivalent circuit models:* The model comprises a combination of RC circuits in series with an internal resistance and an ideal voltage source. However, a single equivalent circuit model cannot describe the battery operation over a large

range of SoC and temperature, [13]. Consequently, an individual parametrisation for various operating conditions (temperature, SoC) is required.

- *Black/grey box techniques:* Data-based modelling approaches offer a versatile structure for the identification of nonlinear systems while the real-time application is easily possible, e. g. [5].

Recent publications have addressed modelling structures for HEV calibration: In [13] a phenomenological model based on an equivalent circuit model with varying parameters is presented. The model parameters are optimised based on measured data using a genetic algorithm. Another interesting approach using state-space model structures with additional hysteresis and filter states is described in [21].

In the automotive industry, local model networks (LMNs) are a widely used concept, e. g. [10, 20, 12]. These models interpolate between different local models, each valid in a certain operating regime, see also e. g. [19, 9]. They offer a versatile structure for the identification of nonlinear dynamic systems and the incorporation of prior (physical) knowledge is easily possible due to the transparency of the LMN architecture. In the sequel some important design aspects of the proposed training algorithm are formulated:

- *Computational speed:* Due to the large number of data in dynamic system identification, a low computational effort is favourable.
- *Incorporation of prior knowledge:* The integration of electro-chemical process knowledge about the cell helps to reduce the complexity of the optimisation algorithm.
- *Robustness/repeatability:* In order to obtain repeatable and robust results, the model must not depend on a random initialisation of parameters.
- *Interpretability:* The architecture of the local model network allows an interpretation of the local models as a local linearisation of the process.

Based on [11] (and [14] respectively), the present paper is focused on the adaptation and extension of LMN structures for Lithium Ion power cell identification for the purpose of SoC estimation.

The remainder of this paper is structured as follows: In Section 2 SoC determination in general and SoC estimation using LMNs is discussed. The architecture of the LMN and the training algorithm are reviewed in Section 3. The associated experiment design is described in Section 4. Using real measurement data, the results of the proposed model structure are highlighted in Section 5.

2 SoC estimation using local model networks

Basically there are two practical approaches how to determine the SoC in a mobile battery, [22]: One is the *relative* SoC determination where an initial SoC is adjusted by taking the time integral of the current:

$$SoC(t) = SoC_0 + \int_{\tau=0}^{t} \frac{\eta_i(i)i(t)}{C_n} d\tau \tag{1}$$

where SoC_0 denotes the initial SoC, $i(t)$ the instantaneous cell current, C_n the nominal cell capacity and $\eta_i(i)$ is the coulombic efficiency. The drawbacks of this method are that the initial SoC has to be known and that the relative SoC determination becomes unreliable when operated in this mode for an extended time. Additionally, the internal resistance of the battery causes thermal energy losses upon (dis-)charging.

Secondly, it is possible to use the *open circuit voltage* (OCV) of a battery cell for an *absolute* SoC-estimation. Since the open circuit voltage is the only measurable battery-intrinsic variable, this approach is more precise in most cases. Unfortunately, it is not possible to directly determine the SoC when the unit is under operation, due to a hysteresis between the charging and discharging voltage profile which depends on the load current. In Fig. 1 the OCV-SoC characteristics and the hysteresis between charging and discharging is depicted.

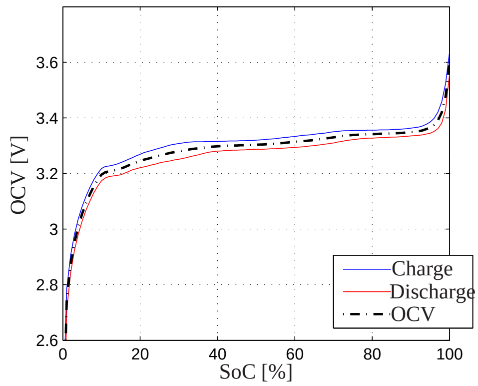

Figure 1: OCV measurement during charging and discharging

SoC *estimation* is typically based on a nonlinear model using Kalman filter theory. The nonlinear model describes the dynamic behaviour of the terminal voltage in dependance of the charge/discharge current $i_{load}(t)$ and other factors like e. g. SoC. The SoC observer is based on a combination of the (relative) SoC model (1) and the terminal voltage model, see

ISBN: 978-1-61804-085-5

Fig. 2. Thus, the SoC correction is obtained from a comparison of the *actual* terminal voltage $U(t)$ to the output of the model.

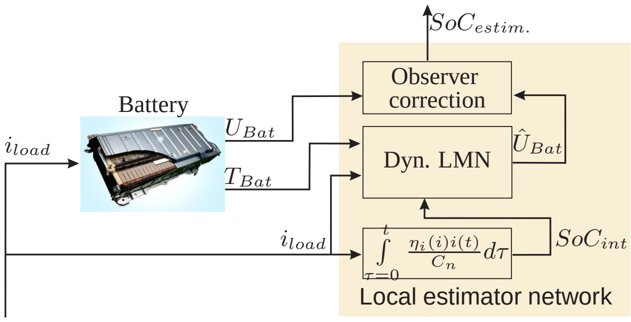

Figure 2: Schematics of SoC observer architecture

In combination with the proposed LMN different observer structures can be used, where the architecture and interpretability of the local models as a local linearisation of the process helps to reduce the model/observer complexity. These observer structures include e.g.:

- *Extended Kalman Filter:* The idea of the extended Kalman filter (EKF) is to apply conventional Kalman filtering to a nonlinear system. The filter gain is computed using the local Jacobian of the nonlinear model. The main disadvantage of this strategy is that the filter gains cannot be precomputed since they depend on data (local linearisation), see e. g. [26, 21].
- *Fuzzy observer:* Each of the local models in an LMN is a linear time-invariant dynamic system. The fuzzy observer for each linear local state space model uses standard Kalman filter theory. Linear combinations of the local filters are used to derive a global filter, [25]. The local observers are time-invariant, which greatly reduces the computational complexity of the global filter.
- *Interacting multiple models (IMM) algorithm:* The multiple model approach accounts for techniques, where the underlying dynamics are linear, but can follow one of several linear models. The basic idea of the multiple model approach is then to run r different linear Kalman filters in parallel, each corresponding to a separate model, [18].

3 Local model network construction

In this section, the architecture and optimisation of the proposed LMN is shortly reviewed. The LMN interpolates between different local models, each valid in a certain region of the input space. Thus the battery cell model is based on a partitioning into several local operating regimes, represented by the dominant influence e. g. SoC, temperature, etc. This strategy allows to capture the highly nonlinear dynamic complexity in a computationally efficient way.

Each local model of the LMN - indicated by subscript i - consists of two parts: The *validity function* $\Phi_i(\tilde{\boldsymbol{x}}(k))$ and its *model parameter vector* $\boldsymbol{\theta}_i$. Thereby, Φ_i defines the region of validity of the i-th local model.

The *local* estimate for the output is obtained by

$$\hat{y}_i(k) = \boldsymbol{x}^T(k)\boldsymbol{\theta}_i, \tag{2}$$

where $\boldsymbol{x}^T(k)$ denotes the regressor vector. In dynamic system identification, the regressor vector $\boldsymbol{x}(k)$ comprises past system inputs and outputs.

All local estimations $\hat{y}_i(k)$ are used to form the global model output $\hat{y}(k)$ by weighted aggregation

$$\hat{y}(k) = \sum_{i=1}^{M} \Phi_i(k)\hat{y}_i(k), \tag{3}$$

where

$$\Phi_i(k) = \Phi_i(\tilde{\boldsymbol{x}}(k)) \tag{4}$$

and M denotes the number of local linear models. Thereby, the elements in $\tilde{\boldsymbol{x}}(k)$ span the so-called partition space and are chosen on the basis of prior knowledge about the process and the expected structure of its nonlinearities. Thus, the dimension of the partition space and furthermore the complexity of the optimisation problem can thus be reduced dramatically, see also [20].

The computation of the validity functions Φ_i is based on a logistic discriminant tree. In Fig. 3 a model tree with three local models is depicted. Each node corresponds to a split of the partition space into two parts and the free ends of the branches represent the actual local models with their parameter vector $\boldsymbol{\theta}_i$ and their validity functions Φ_i. The overall nonlinear model thus comprises M local models and $M-1$ nodes which determine their regions of validity.

For the representation of the discriminant function in the d-th node a logistic sigmoid activation function is chosen, c. f. [4]:

$$\varphi_d(\tilde{\boldsymbol{x}}(k)) = \frac{1}{1+\exp(-a_d(\tilde{\boldsymbol{x}}(k)))} \tag{5}$$

with

$$a_d(\tilde{\boldsymbol{x}}(k)) = \begin{bmatrix}1 & \tilde{\boldsymbol{x}}^T(k)\end{bmatrix} \begin{bmatrix}\psi_{d0} \\ \tilde{\boldsymbol{\psi}}_d\end{bmatrix}. \tag{6}$$

ISBN: 978-1-61804-085-5

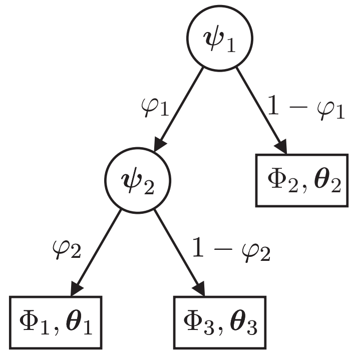

Figure 3: Logistic discriminant tree

Here, $\tilde{\psi}_d^T = \left[\psi_{d1} \ldots \quad \psi_{dp}\right]$ denotes the weight vector and ψ_{d0} is called bias term. The discriminant functions φ_d are used to calculate the validity functions Φ_i, c. f. [24].

The validity functions for the layout in Fig. 3 are obtained by

$$\Phi_1 = \varphi_1\varphi_2, \tag{7}$$

$$\Phi_2 = 1 - \varphi_1, \tag{8}$$

$$\Phi_3 = \varphi_1(1 - \varphi_2). \tag{9}$$

An incremental model construction allows to gradually increase the complexity of the local model network: When the number of local models M is increased by one, the *worst* local model (indexed by l) of the logistic discriminant tree in Fig. 3 is replaced by a new node and two adjoining local models are appended, see Fig. 4. On the one hand this strategy allows a proper initialisation of the new model parameters while on the other hand the computational demand is low.

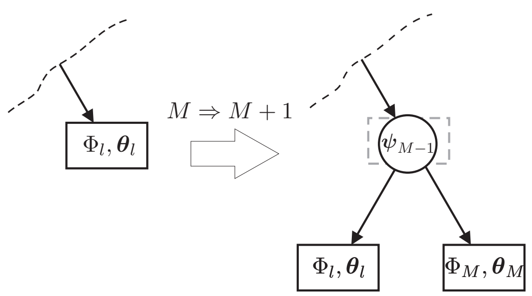

Figure 4: Incremental tree construction

In order to reduce the computational demand, only the weight vector of the new node ψ_{M-1} is optimised while all other weight vectors are retained.

An important topic in nonlinear system identification with local model networks is the interpretability of the local models, see e. g. [3, 15, 1]. Only consequent parameters obtained by local estimation (weighted least squares) allow the interpretation of the consequent parameters as a local linearisation of the nonlinear system, [1]. In order to obtain an interpretable model structure for the proposed LMN, the following cost function is chosen for the optimisation of the two new local models and the weight vector of the new node:

$$\begin{aligned} J &= \frac{1}{2}\sum_{k=1}^{N} \Phi_l(k)\left[y(k) - \hat{y}_l(k)\right]^2 + \\ &\quad +\Phi_M(k)\left[y(k) - \hat{y}_M(k)\right]^2 \\ &= \frac{1}{2}\sum_{k=1}^{N} e_l^2(k) + e_M^2(k), \end{aligned} \tag{10}$$

where

$$e_l(k) = \sqrt{\Phi_l(k)}\left[y(k) - \hat{y}_l(k)\right] \tag{11}$$

and

$$e_M(k) = \sqrt{\Phi_M(k)}\left[y(k) - \hat{y}_M(k)\right] \tag{12}$$

are the *weighted* local prediction errors of the adjoining models l and M, respectively. In (10) N defines the number of training data.

Note that the particular choice of (10) aims at a *locally* weighted least squares optimisation of the consequent parameters so that local interpretability is conserved.

If in (10) all observations $k = 1, \ldots, N$ are collected in error vectors $\boldsymbol{e}_l$ and $\boldsymbol{e}_M$ the cost functions can be rewritten as:

$$J = \frac{1}{2}\left[\boldsymbol{e}_l^T\boldsymbol{e}_l + \boldsymbol{e}_M^T\boldsymbol{e}_M\right] \tag{13}$$

Using the first-order approximation of the expressions in equation (13) and taking the derivative with respect to the parameters $\boldsymbol{\theta}_l$, $\boldsymbol{\theta}_M$ and $\boldsymbol{\psi}_{M-1}$ a set of linear equations is obtained for the iterative optimisation of (10):

$$\boldsymbol{R}^{(n)}\begin{bmatrix}\Delta\boldsymbol{\theta}_l \\ \Delta\boldsymbol{\theta}_M \\ \Delta\boldsymbol{\psi}_{M-1}\end{bmatrix} + \boldsymbol{G}^{(n)} = 0, \tag{14}$$

where

$$\boldsymbol{G}^{(n)} = \left.\begin{bmatrix} \frac{\partial \boldsymbol{e}_l}{\partial \boldsymbol{\theta}_l}^T \boldsymbol{e}_l \\ \frac{\partial \boldsymbol{e}_M}{\partial \boldsymbol{\theta}_M}^T \boldsymbol{e}_M \\ \frac{\partial \boldsymbol{e}_l}{\partial \boldsymbol{\psi}_{M-1}}^T \boldsymbol{e}_l + \frac{\partial \boldsymbol{e}_M}{\partial \boldsymbol{\psi}_{M-1}}^T \boldsymbol{e}_M \end{bmatrix}\right|_{(n)}. \tag{15}$$

In (14) matrix $\boldsymbol{R}^{(n)}$ is defined as

$$\boldsymbol{R}^{(n)} = \left[\boldsymbol{\Xi}_l^{(n)}\right]^T \boldsymbol{\Xi}_l^{(n)} + \left[\boldsymbol{\Xi}_M^{(n)}\right]^T \boldsymbol{\Xi}_M^{(n)}. \tag{16}$$

with

$$\Xi_l^{(n)} = \left[\frac{\partial \boldsymbol{e}_l}{\partial \boldsymbol{\theta}_l} \quad \mathbf{0} \quad \frac{\partial \boldsymbol{e}_l}{\partial \boldsymbol{\psi}_{M-1}} \right] \Bigg|_{(n)} \tag{17}$$

and

$$\Xi_M^{(n)} = \left[\mathbf{0} \quad \frac{\partial \boldsymbol{e}_M}{\partial \boldsymbol{\theta}_M} \quad \frac{\partial \boldsymbol{e}_M}{\partial \boldsymbol{\psi}_{M-1}} \right] \Bigg|_{(n)} . \tag{18}$$

4 Design of experiments

The proposed concepts are validated using real measurement data from a high power Lithium Ion cell. An important prerequisite for data-based modelling approaches is a suitable experiment design. In general, the target of the design of experiments (DoE) is to generate informative data while the experimentation effort is reduced. Thus, the experiment design can be understood as a compromise between experimentation effort, reliability and accuracy under the specific loads and environmental conditions.

For cell modelling, the whole operating range (cell current, SoC) of the cell has to be covered and the model must be accurate for a highly dynamic excitation. One of the main challenges regarding the experiment design, is that the SoC excitation (and the operating range) directly depends on the excitation signal of the cell current, see (1). In the present paper, the desired SoC profile is obtained from a multitude of short locally optimised input sequences (see Fig. 5):

1. The local optimisation of the excitation signal (cell current) is based on a simple linear cell model. The target of such a *model based* DoE is that parameters belonging to a specific model structure can be estimated from measured data with minimal variance, see e. g. [23, 8].

2. In order to obtain the desired SoC profile, the amount of charge to be drawn from or fed to the cell is mathematically enforced using a constrained optimisation algorithm.

The appropriate sequential arrangement of the local excitation sequences then yields the desired SoC profile. One of the local training data sequences (a section of the complete training data) is depicted in Fig. 5. The complete training data record is shown in Fig. 6, where the initial value of "Charge [Ah]" corresponds to 80% SoC. The nominal capacity of the power cell is 2.3Ah and the nominal voltage 3.3V, respectively. Accordingly, the SoC operating range of the training data is between 20% and 80% SoC.

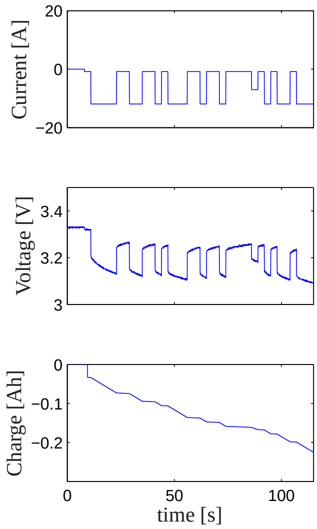

Figure 5: Training data section (zoom)

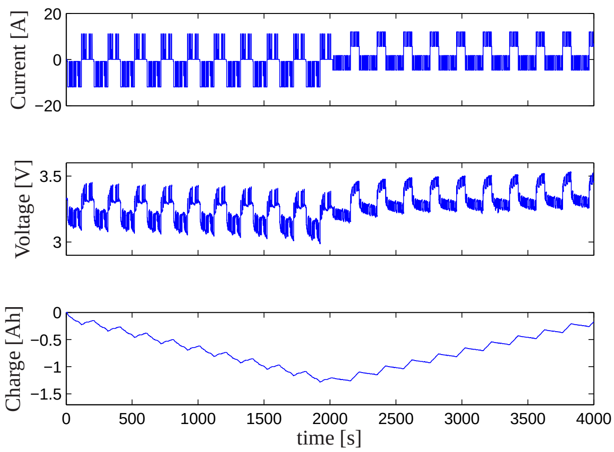

Figure 6: Training data record

5 Modelling and results

5.1 Extended model structure

In this section, the identification of a Lithium Ion power cell is presented. The input into the model is the cell current $i(k)$ and the model output is the cell terminal voltage $u(k)$. The state of charge is only used for the partitioning of the LMN. For the feasibility study presented in this paper, the cell temperature is kept constant.

In order to take into account special effects such as hysteresis and relaxation, the structure of the LMN is adapted/extended:

1. The values for the resistance and capacitance of a cell model are functions of the direction of current and SoC, [13]. Thus, separate models for charge and discharge are constructed to approximate the voltage hysteresis. The architecture of LMNs allows an easy integration of this dependency using a user-defined pre-partitioning based on the current direction $\mathrm{sign}(i)$.

2. In [21], large time constants which describe the relaxation effect are implemented as a low-pass filter on $i(k)$. Accordingly, an additional input

$$v = \mathrm{filt}(i) \tag{19}$$

for the LMN is used in this work. The filt-operator in (19) represents a low-pass filter with zero dc gain. Here, zero dc gain ensures that the influence of the additional input vanishes after a rest period so that the model output converges to OCV, c. f. [21].

5.2 Results

The performance of the LMN is highlighted using real measurement data from a Lithium Ion power cell, see Fig. 6. The training of the LMN using the algorithm presented in Section 3 results in an LMN with nine local linear models. In Fig. 7 a comparison of measured and simulated model output at the training data is depicted. It is clearly visible that the LMN accurately describes the nonlinear behaviour of the cell while the SoC is varied in a wide range. A closer look at comparison between measured and simulated output is presented in Fig. 8.

In order to prove the generalisation capabilities of the proposed LMN validation data were recorded, see Fig. 9. Here, the current profile was taken from [13] and adjusted in a way that the desired SoC operating range is covered. Again, the initial value of ”Charge [Ah]” corresponds to 80% SoC. The simulated model output of the LMN at the validation data is depicted

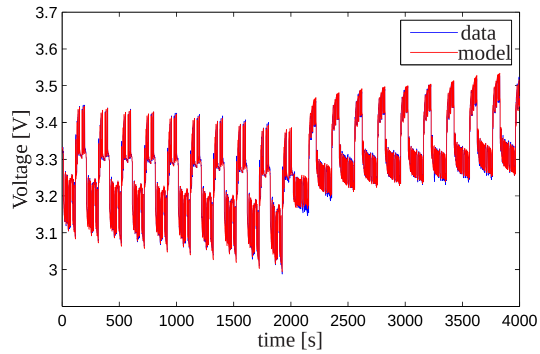

Figure 7: Comparison of measured and simulated model output (training data)

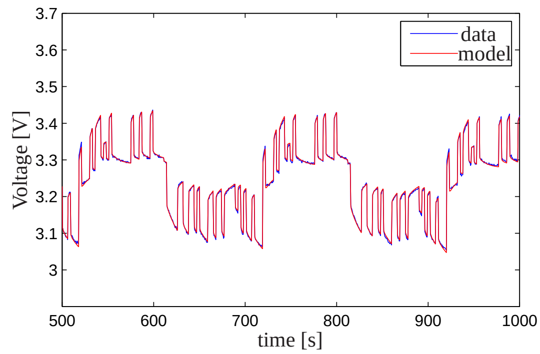

Figure 8: Comparison of measured and simulated model output (training data) - zoom

in Fig. 10. Obviously, the model accurately describes the nonlinear dynamic behaviour of the Lithium Ion power cell.

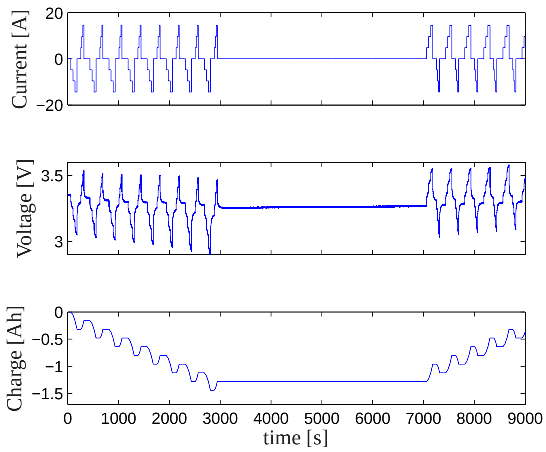

Figure 9: Validation data record

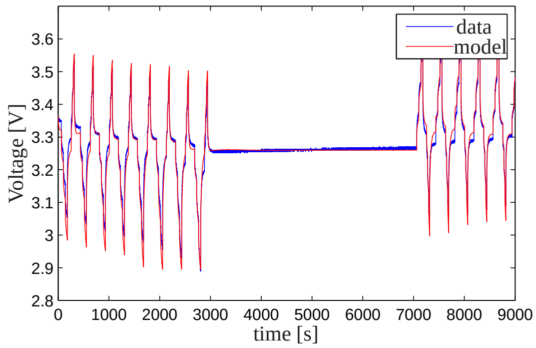

Figure 10: Comparison of measured and simulated model output (validation data)

6 Conclusion

The work described in the present paper shows the nonlinear system identification of a Lithium Ion power cell for the purpose of SoC estimation using LMNs. Such a model describes the dynamic behaviour of the terminal voltage in dependance of the charge/discharge current. For the application in HEVs, the model must be accurate for a highly dynamic excitation in combination with high C-rates. In this paper, appropriate SoC observer structures for LMNs are discussed and the LMN construction/optimisation algorithm is reviewed. The performance of the LMN is highlighted using real measurement data from the Lithium Ion power cell and the simulation results show that the model accurately describes the nonlinear dynamic behaviour at the generalisation data. Future work will be focused on the SoC estimation using the proposed LMN and the integration of the temperature dependency in the modelling framework.

Acknowledgements: This work was supported by the Christian Doppler Research Association and AVL List GmbH, Graz.

References:

[1] J. Abonyi and R. Babuska. Local and global identification and interpretation of parameters in takagi-sugeno fuzzy models. In *Fuzzy Systems, 2000. FUZZ IEEE 2000. The Ninth IEEE International Conference on*, volume 2, pages 835 – 840 vol.2, 2000.

[2] Pankaj Arora, Marc Doyle, Antoni S. Gozdz, Ralph E. White, and John Newman. Comparison between computer simulations and experimental data for high-rate discharges of plastic lithium-ion batteries. *Journal of Power Sources*, 88(2):219 – 231, 2000.

[3] Robert Babuska. *Fuzzy Modeling for Control*. Kluwer Academic Publishers, Norwell, MA, USA, 1998.

[4] Christopher M. Bishop. *Neural networks for pattern recognition*. Oxford University Press, USA, 1995.

[5] M. Charkhgard and M. Farrokhi. State-of-charge estimation for lithium-ion batteries using neural networks and ekf. *Industrial Electronics, IEEE Transactions on*, 57(12):4178 –4187, dec. 2010.

[6] J. Chatzakis, K. Kalaitzakis, N.C. Voulgaris, and S.N. Manias. Designing a new generalized battery management system. *Industrial Electronics, IEEE Transactions on*, 50(5):990–999, Oct. 2003.

[7] Parthasarathy M. Gomadam, John W. Weidner, Roger A. Dougal, and Ralph E. White. Mathematical modeling of lithium-ion and nickel battery systems. *Journal of Power Sources*, 110(2):267 – 284, 2002.

[8] G.C. Goodwin and R.L. Payne. *Dynamic System Identification: Experiment Design and Data Analysis*, volume 136 of Mathematics in Science and Engineering. Academic Press, 1977.

[9] G. Gregorcic and G. Lightbody. Local Model Network Identification With Gaussian Processes. *Neural Networks, IEEE Transactions on*, 18(5):1404 –1423, sept. 2007.

[10] M. Hafner, M. Schler, O. Nelles, and R. Isermann. Fast neural networks for diesel engine control design. *Control Engineering Practice*, 8(11):1211 – 1221, 2000.

[11] C. Hametner and S. Jakubek. Neuro-fuzzy modelling using a logistic discriminant tree. *American Control Conference, 2007. ACC '07*, pages 864–869, July 2007.

[12] C. Hametner and S. Jakubek. Combustion engine modelling using an evolving local model network. In *Proceedings of the 2011 International Conference on Fuzzy Systems (FUZZ IEEE 2011)*, June 2011.

[13] Yiran Hu, Benjamin J. Yurkovich, Stephen Yurkovich, and Yann Guezennec. Electro-thermal battery modeling and identification for automotive applications. *ASME Conference Proceedings*, 2009(48937):233–240, 2009.

[14] S. Jakubek and C. Hametner. Identification of Neurofuzzy Models Using GTLS Parameter Estimation. *Systems, Man, and Cybernetics, Part B: Cybernetics, IEEE Transactions on*, 39(5):1121–1133, Oct. 2009.

[15] T. A. Johansen, R. Shorten, and R. Murray-Smith. On the Interpretation and Identification of Dynamic Takagi-Sugeno Fuzzy Models. *IEEE Transactions on Fuzzy Systems*, 8(3):297–313, 2000.

[16] R. Klein, N.A. Chaturvedi, J. Christensen, J. Ahmed, R. Findeisen, and A. Kojic. State estimation of a reduced electrochemical model of a lithium-ion battery. In *American Control Conference (ACC), 2010*, pages 6618 –6623, 30 2010-july 2 2010.

[17] D. Lim and A. Anbuky. A can-based battery management network: design, analysis, modelling and simulation. *Factory Communication Systems, 2004. Proceedings. 2004 IEEE International Workshop on*, pages 291–295, Sept. 2004.

[18] E. Mazor, A. Averbuch, Y. Bar-Shalom, and J. Dayan. Interacting multiple model methods in target tracking: a survey. *Aerospace and Electronic Systems, IEEE Transactions on*, 34(1):103 –123, jan. 1998.

[19] R. Murray-Smith and T. A. Johansen. *Multiple Model Approaches to Modelling and Control*. Taylor & Francis, 1997.

[20] O. Nelles. *Nonlinear System Identification*. Springer Verlag, 1st edition, 2002.

[21] Gregory L. Plett. Extended Kalman filtering for battery management systems of LiPB-based HEV battery packs: Part 2. Modeling and identification. *Journal of Power Sources*, 134(2):262 – 276, 2004.

[22] V Pop, H J Bergveld, P H L Notten, and P P L Regtien. State-of-the-art of battery state-of-charge determination. *Measurement Science and Technology*, 16(12):R93–R110, 2005.

[23] Luc Pronzato. Optimal experimental design and some related control problems. *Automatica*, 44(2):303–325, 2008.

[24] P. Pucar and M. Millnert. Smooth hinging hyperplanes - an alternative to neural networks. In *Proceedings of the 3rd ECC*, 1995.

[25] R. Senthil, K. Janarthanan, and J. Prakash. Nonlinear State Estimation Using Fuzzy Kalman Filter. *Industrial & Engineering Chemistry Research*, 45(25):8678–8688, 2006.

[26] Amir Vasebi, Maral Partovibakhsh, and S. Mohammad Taghi Bathaee. A novel combined battery model for state-of-charge estimation in lead-acid batteries based on extended kalman filter for hybrid electric vehicle applications. *Journal of Power Sources*, 174(1):30 – 40, 2007. Hybrid Electric Vehicles.